Revision 1

Supplementary Material

Thermoelasticity of Tremolite Amphibole: Geophysical Implications

Ye Peng[1], Mainak Mookherjee
Earth Materials Laboratory, Department of Earth, Ocean and Atmospheric Science,
Florida State University, Tallahassee, FL 32306, USA
[1]*corresponding author*: yp16b@my.fsu.edu

Section I

The temperature dependence of the thermodynamic parameters at zero-pressure is discussed in the main draft. Here, we present additional analysis of the *P-V-T* data using two distinct formalisms: high-temperature Birch-Murnaghan (HTBM) equation of state (EOS) and Mie-Grüneisen-Debye (MGD) EOS (Anderson, 1984; Fei et al., 1992; Nishihara et al., 2005; Litasov et al., 2007).

High-temperature Birch-Murnaghan equation of state

In high-temperature Birch-Murnaghan (HTBM) equation of state, the *P-V-T* data is described as

$$P = \frac{3}{2} K_T \left[\left(\frac{V_{0T}}{V}\right)^{\frac{7}{3}} - \left(\frac{V_{0T}}{V}\right)^{\frac{5}{3}} \right] \left\{ 1 + \frac{3}{4} (K_T{}' - 4) \left[\left(\frac{V_{0T}}{V}\right)^{\frac{2}{3}} - 1 \right] \right\} \quad (1)$$

where

$$K_T = K_{T0} \left(\frac{V_{0T}}{V_0}\right)^{-\delta_T} \quad (2)$$

and

$$V_{0T} = V_0 \exp\left(\int_{T0}^{T} \alpha \, \mathrm{d}T \right) \quad (3)$$

Since the thermal expansion coefficient can be empirically represented by $\alpha = a_0 + a_1 T$, the eq. (3) can be rewritten as

$$V_{0T} = V_0 \exp\left[a_0 (T - T_0) + \frac{a_1}{2} (T^2 - T_0^2) \right] \quad (4)$$

In the HBTM EOS formalism, there are six thermoelastic parameters: the isothermal bulk modulus at standard temperature and pressure (STP) (K_{T0}), the unit-cell volume at STP (V_0), the pressure derivative of bulk modulus ($K_T{}'$), the second Grüneisen parameter (δ_T), and the thermal expansivity parameters (a_0 and a_1) (**Supplementary Table 5**). In this study, the standard temperature and pressure (STP) indicate 300 K and 0 GPa. Based on our analysis of the *P-V-T* data, we find that the root-mean-square (RMS) misfit from HTBM EOS formalism is ~0.12 GPa. The values of the K_{T0}, V_0, and $K_T{}'$ are consistent with those derived from the isothermal fit at room-temperature data (**Table 1**). The thermal expansion coefficient α, represented by a_0 and a_1, also agrees well with the α determined at STP ($\alpha^{LDA} = 2.7\times10^{-5}$ K^{-1} and $\alpha^{GGA} = 2.5\times10^{-5}$ K^{-1}). Similarly, the second Grüneisen parameter δ_T^{LDA} agrees with that determined directly from the temperature dependence of K_T, which is 3.33. The second Grüneisen parameter, $\delta_T < K_T{}'$ ($\delta_T^{LDA} - K'^{LDA}_T$ = -1.7 and $\delta_T^{GGA} - K'^{GGA}_T$ = -4.6), and the

large non-zero values indicate that the thermal pressure (P_{th}) for tremolite is strongly sensitive to the volume (Anderson, 1999).

Mie-Grüneisen-Debye equation of state

In the MGD EOS formalism, the pressure at a given volume and temperature can be expressed as the sum of static pressure and thermal pressure:

$$P(V,T) = P(V,T_0) + P_{th}(V,T) \quad (5)$$

The static pressure is described by a third-order Birch Murnaghan equation of state, and the thermal pressure is expressed by

$$P_{th}(V,T) = \frac{\gamma}{V}[E_{th}(V,T) - E_{th}(V,T_0)] \quad (6)$$

where the first Grüneisen parameter γ is described as a function of volume

$$\gamma(V) = \gamma_0 \left(\frac{V}{V_0}\right)^q \quad (7)$$

and the Debye energy is

$$E_{th}(V,T) = \frac{9nRT}{(\Theta_T/T)^3}\int_0^{\Theta_T/T} \frac{t^3}{e^t-1}\mathrm{d}t \quad (8)$$

where n is the number of atoms in the formula unit, R is the gas constant, and Θ_T is the Debye temperature which is described as

$$\Theta_T(V) = \Theta_{T0}\left(\frac{V}{V_0}\right)^{-\gamma} \quad (9)$$

Thus, in the MGD EOS formalism, there are six thermoelastic parameters: the isothermal bulk modulus at STP (K_{T0}), the unit-cell volume at STP (V_0), the pressure derivative of bulk modulus ($K_T{}'$), the first Grüneisen parameter at STP (γ_0), the dimensionless constant (q), and the Debye temperature at STP (Θ_{T0}) (**Supplementary Table 5**). Based on our analysis of the *P-V-T* data, we find that the RMS misfit from MDG EOS formalism is ~0.09 GPa. Again, the values of the K_{T0}, V_0, and $K_T{}'$ do not exhibit significant variation across the two formalisms. The first Grüneisen parameters are similar as those determined based on $\gamma = \frac{\alpha K_T V}{C_V}$ at STP ($\gamma^{LDA} = 0.86$ and $\gamma^{GGA} = 0.71$). The Debye temperatures from the MGD EOS formalism (**Supplementary Table 5**) are comparable with the Θ_T ($\Theta_T^{LDA} = 650.6$ K and $\Theta_T^{GGA} = 625.4$ K) determined from average seismic velocities ($\bar{v}$) as:

$$\Theta_T = \frac{\hbar\bar{v}}{k_B}\left(\frac{6\pi^2 nZ}{V}\right)^{\frac{1}{3}} \quad (10)$$

where, the $\hbar$ is the reduced Planck constant, k_B is the Boltzmann constant, n is the number of atoms in the formula unit, Z is the number of formula units in the unit-cell, and V is the volume of the unit-cell. The average seismic velocity ($\bar{v}$) is expressed as a function of compressional (V_P) and shear (V_S) wave velocity

$$\bar{v} = \left[3\left(\frac{1}{V_P^3} + \frac{2}{V_S^3}\right)\right]^{\frac{1}{3}} \quad (11)$$

The large volume dependence of thermal pressure P_{th} in the MGD EOS formalism yields $q < 0$, with q^{LDA} = -0.7 and q^{GGA} = -3.6. An alternate check on the determination of q could be based on the definition of q, i.e., $\left(\frac{\partial \ln\gamma}{\partial \ln V}\right)_T$ where, $\gamma = \frac{\alpha K_T V}{C_V}$ (Bassett et al., 1968; Anderson, 1984; Anderson and Yamamoto, 1987; Bina and Helffrich, 1992), thus

$$q = \left(\frac{\partial \ln\gamma}{\partial \ln V}\right)_T = \left[\frac{\partial(\ln\alpha+\ln K_T+\ln V-\ln C_V)}{\partial \ln V}\right]_T = \delta_T - K_T{}' + 1 - \left(\frac{\partial \ln C_V}{\partial \ln V}\right)_T \quad (12)$$

Assuming the last term, i.e., $\left(\frac{\partial \ln C_V}{\partial \ln V}\right)_T$ in eq. (12) is negligible, the q will be consistent between the HTBM and the MGD EOS formalisms.

In most earlier studies on silicate mineral phases, q is often assumed to be 1 and this assumption implies $\delta_T \approx K_T{}'$. This suggests that P_{th} is not sensitive to volume along an isotherm (Anderson, 1999). In contrast, the thermal pressure (P_{th}) of tremolite has a strong dependence on volume. Since the δ_T describes the temperature effect on the K_T, while the $K_T{}'$ is the pressure dependence of K_T, the relationship of $\delta_T = K_T{}'$also gives us an insight on how the K_T changes along an isochore

$$\left(\frac{\partial K_T}{\partial T}\right)_V = -V\left[\frac{\partial(\alpha K_T)}{\partial V}\right]_T = -\alpha K_T(\delta_T - K_T{}') \quad (13)$$

Thus, K_T is a constant along an isochore when $\delta_T = K_T{}'$ is satisfied. However, K_T of tremolite increases with temperature along the isochore with the $\left(\frac{\partial K_T}{\partial T}\right)_V^{LDA} = 3.6$ MPa/K and $\left(\frac{\partial K_T}{\partial T}\right)_V^{GGA} = 6.5$ MPa/K. It is to be noted that the large non-zero values with $\delta_T < K_T{}'$ are also observed in other mineral phases which include magnesite (Anderson, 1999; Litasov et al., 2008).

Section II

To predict the lithospheric mantle velocity-depth profiles, we used thermoelastic codes (Abers and Hacker, 2016). The thermoelastic parameters for calculating the aggregate velocities and the formalisms used to extend them at high pressures and temperatures are provided in detail (**Table 3**, **Supplementary Table 11**).

Thermoelastic parameters- effect of temperature

The temperature dependence of volume of a mineral phase is captured by a dimensionless parameter, Φ, defined as (Hacker and Abers, 2004):

$$\Phi \equiv \ln\frac{V(T)}{V_0} = \int_{T_0}^{T} \alpha(T)dT \quad (14)$$

where V_0 is the volume of the mineral phase at STP. The thermal expansion coefficient $\alpha(T)$ is defined by a constant a^0 for each mineral phase (Holland and Powell, 1998):

$$\alpha(T) = a^0\left(1 - \frac{10}{\sqrt{T}}\right) \quad (15)$$

Thus, eq. (14) can be rewritten as:

$$\Phi \equiv \int_{T_0}^{T} \alpha(T)dT = a^0\left[(T - T_0) - 20\left(\sqrt{T} - \sqrt{T_0}\right)\right] \quad (16)$$

Thus, temperature dependence of density could also be expressed in terms of Φ as:

$$\rho(T) = \rho_0 e^{-\Phi} \quad (17)$$

where ρ_0 is the density at STP.

The temperature dependence of isothermal bulk modulus $K_T(T)$ can also be expressed in terms of Φ as:

$$K_T(T) = K_{T0}e^{-\delta_T\Phi} \quad (18)$$

where K_{T0} is the isothermal bulk modulus at STP, δ_T is the isothermal second Grüneisen parameter and is related to $\left(\frac{\partial K_T}{\partial T}\right)_P$ (Bina and Helffrich, 1992; Anderson et al., 1992) as:

$$\delta_T \equiv -\frac{1}{\alpha K_T}\left(\frac{\partial K_T}{\partial T}\right)_P = -\left(\frac{\partial \ln K_T}{\partial \ln V}\right)_P = \left(\frac{\partial \ln K_T}{\partial \ln \rho}\right)_P \quad (19)$$

Similarly, the temperature dependence of shear modulus $G(T)$ can also be expressed in terms of Φ as:

$$G(T) = G_0 e^{-\Gamma\Phi} \quad (20)$$

where G_0 is the isothermal shear modulus at STP, and Γ is related to $\left(\frac{\partial G}{\partial T}\right)_P$ (Duffy and Anderson, 1989; Anderson et al., 1992) and defined as:

$$\Gamma \equiv -\frac{1}{\alpha G}\left(\frac{\partial G}{\partial T}\right)_P = -\left(\frac{\partial \ln G}{\partial \ln V}\right)_P = \left(\frac{\partial \ln G}{\partial \ln \rho}\right)_P \quad (21)$$

Thermoelastic parameters- effect of pressure

The pressure dependence of volume and density of a mineral phase is often best described by a finite strain equation of state (Birch, 1978):

$$\frac{P}{K_T} = 3f(1+2f)^{\frac{5}{2}}\left[1+\frac{3}{2}(K'-4)f\right] \quad (22)$$

where f is the Eulerian finite strain, K' is the pressure dependence of isothermal bulk modulus, i.e., $\left(\frac{\partial K_T}{\partial P}\right)_T$.

The density at high pressures can be expressed in terms of f as:

$$\rho(P) = \rho_0(1+2f)^{\frac{3}{2}} \quad (23)$$

Thermoelastic parameters- combined effect of pressure and temperature

The combined effect of pressure and temperature on density can be expressed by combining eq. (17) and eq. (23) as:

$$\rho(P,T) = \frac{\rho(P)}{\rho_0}\rho(T) = \rho_0(1+2f)^{\frac{3}{2}}e^{-\Phi} \quad (24)$$

Similarly, the combined effect of pressure and temperature on bulk modulus can be expressed as:

$$K_T(P,T) = K_{T0}(1+2f)^{\frac{5}{2}}[1+(3K'-5)f]e^{-\delta_T\Phi} \quad (25)$$

and the combined effect of pressure and temperature on shear modulus can be expressed as:

$$\begin{aligned} G(P,T) &= G_0(1+2f)^{\frac{5}{2}}\left\{1+\left[3G'\frac{K_T(T)}{G(T)}-5\right]f\right\}e^{-\Gamma\Phi} \\ &= G_0(1+2f)^{\frac{5}{2}}\left\{1+\left[3G'\frac{K_{T0}e^{-\delta_T\Phi}}{G_0e^{-\Gamma\Phi}}-5\right]f\right\}e^{-\Gamma\Phi} \end{aligned} \quad (26)$$

The thermal expansion coefficient at high pressure and temperature is

$$\alpha(P,T) = \alpha(T)\left[\frac{\rho(P)}{\rho_0}\right]^{-\delta_T} = a^0\left(1-\frac{10}{\sqrt{T}}\right)(1+2f)^{-\frac{3}{2}\delta_T} \quad (27)$$

The adiabatic bulk modulus is

$$\begin{aligned} K_S(P,T) &= K_T(P,T)[1+T\gamma_{th}\alpha(P,T)] \\ &= K_{T0}(1+2f)^{\frac{5}{2}}[1+(3K'-5)f][1+T\gamma_{th}\alpha(P,T)]e^{-\delta_T\Phi} \end{aligned} \quad (28)$$

where γ_{th} is the first isothermal Grüneisen parameter defined by

$$\gamma_{th} \equiv \frac{\alpha V K_T}{C_V} \equiv \frac{\alpha V K_S}{C_P} \quad (29)$$

Aggregate properties

For a rock consisting of *n* mineral phases, the density can be expressed as:

$$\rho = \sum_{i=1}^{n} \nu_i \rho_i \quad (30)$$

where ρ_i and ν_i are the density and volume proportion of each mineral phase, respectively.

The aggregate bulk and shear modulus of the rock are calculated by Hashin-Shtrikman average (Hashin and Shtrikman, 1962). The bulk modulus can be expressed as:

$$K = \frac{\left(K_1 + \frac{A_1}{\alpha_1 A_1 + 1}\right) + \left(K_n + \frac{A_n}{\alpha_n A_n + 1}\right)}{2} \quad (31)$$

where, the K_1 is the softest bulk modulus, K_n is the stiffest bulk modulus, and

$$\alpha_1 = -\frac{3}{3K_1 + 4G_1}$$

$$\alpha_n = -\frac{3}{3K_n + 4G_n}$$

$$A_1 = \sum_{i=2}^{n} \frac{\nu_i}{\frac{1}{K_i - K_1} - \alpha_1}$$

$$A_n = \sum_{i=1}^{n-1} \frac{\nu_i}{\frac{1}{K_i - K_n} - \alpha_n} \quad (32)$$

The shear modulus is analogous:

$$G = \frac{\left(G_1 + \frac{1}{2\beta_1} \frac{B_1}{B_1 + 1}\right) + \left(G_n + \frac{1}{2\beta_n} \frac{B_n}{B_n + 1}\right)}{2} \quad (33)$$

where, the G_1 is the softest shear modulus, G_n is the stiffest shear modulus, and

$$\beta_1 = \frac{\alpha_1 (K_1 + 2G_1)}{5G_1}$$

$$\beta_n = \frac{\alpha_n (K_n + 2G_n)}{5G_n}$$

$$B_1 = \sum_{i=2}^{n} \frac{\nu_i}{\frac{2}{G_i - G_1} - \beta_1}$$

$$B_n = \sum_{i=1}^{n-1} \frac{\nu_i}{\frac{2}{G_i - G_n} - \beta_n} \quad (34)$$

The compressional and shear seismic wave velocities at given temperature and pressure are then calculated as

$$V_P = \sqrt{\frac{K_S + \frac{4}{3} G}{\rho}} \quad (35)$$

and

$$V_S = \sqrt{\frac{G}{\rho}} \quad (36)$$

Supplementary Tables

Supplementary Table 1. The total energy as a function of increasing cut-off energy (E_{cutoff}) at a constant volume of 870 Å^3 using LDA. The K-points remain unchanged.

K-Points	E_{cutoff}(eV)	Energy (eV)
6	500	-647.28
6	600	-647.48
6	700	-647.71
6	800	-647.79
6	900	-647.80
6	1000	-647.81
6	1100	-647.82

Supplementary Table 2. The total energy as a function of increasing K-points at the constant volume of 870 Å^3 using LDA. The cut-off energy of 800 eV remain unchanged.

K-points	E_{cutoff}(eV)	Energy (eV)
2	800	-647.68
6	800	-647.79
20	800	-647.79
36	800	-647.79

Supplementary Table 3. The difference of elastic properties due to different energy cut-offs at three distinct volumes using LDA. The difference is defined by $\Delta M = (M^{1000eV} - M^{800eV})/M^{800eV}$ x 100%, where the M represents the elastic properties.

V [Å^3]	$P_{0\,K}$ [GPa]	$P_{300\,K}$ [GPa]	C_{11} [%]	C_{22} [%]	C_{33} [%]	C_{12} [%]	C_{13} [%]	C_{23} [%]	C_{44} [%]	C_{55} [%]	C_{66} [%]	C_{15} [%]	C_{25} [%]	C_{35} [%]	C_{46} [%]	K_{VRH} [%]	G_{VRH} [%]	V_P [%]	V_S [%]
800	10.00	10.62	0.1	0.0	0.1	0.1	0.1	0.0	0.0	0.1	0.0	-1.7	-4.1	-0.3	-0.1	0.1	0.0	0.03	0.02
850	2.66	3.75	0.0	0.0	0.1	0.2	0.4	0.0	-0.1	0.0	0.1	-1.0	-0.3	0.0	0.2	0.1	-0.1	0.02	-0.03
870	0.49	1.61	0.2	-0.2	0.3	-0.1	0.0	0.0	0.0	0.0	0.0	0.3	1.0	0.1	0.7	0.0	0.1	0.03	0.04

Supplementary Table 4. The thermal expansion coefficient (α) as a function of pressure at 300 K.

P [GPa]	0	1	2	3	4	5	6	7	8	9	10	$\alpha(P) = \frac{1}{2}\alpha_0''P^2 + \alpha_0'P + \alpha_0$	
												α_0'' [K^{-1}GPa^{-2}]	α_0' [K^{-1}GPa^{-1}]
α^{LDA} [x10^{-5} K^{-1}]	2.70	2.60	2.53	2.47	2.42	2.37	2.33	2.30	2.27	2.25	2.23	7.5x10^{-8}	-8.4x10^{-7}
α^{GGA} [x10^{-5} K^{-1}]	2.50	2.42	2.35	2.30	2.25	2.21	2.18	2.15	2.13	2.11	2.09	6.6x10^{-8}	-7.3x10^{-7}

Supplementary Table 5. Thermoelastic parameters of tremolite from the high-temperature Birch-Murnaghan (HTBM) equation of state and the Mie-Grüneisen-Debye (MGD) equation of state.

		LDA		GGA	
Parameters	Unit	HTBM	MGD	HTBM	MGD
K_0	GPa	79.9	80.2	64.9	65.1
K_0'		5.2	5.2	6.8	6.7
V_0	$Å^3$	888.1	887.5	958.6	958.1
a_0	$x10^{-5}$ K^{-1}	2.5	-	2.7	-
a_1	$x10^{-8}$ K^{-2}	0.6	-	0.3	-
δ_T		3.5	-	2.2	-
γ_0		-	0.7	-	0.6
q		-	-0.7	-	-3.6
Θ_{T0}	K	-	566.1	-	589.8
RMS misfit	GPa	0.12	0.09	0.08	0.06

Supplementary Table 6. Pressure dependence of polyhedral volumes and bond lengths of tremolite at 300 K.

Pressure	Polyhedral Volume							Average bond distance within the polyhedral							Hydroxyl bond
$P_{300\,K}$	A(vacant)	B	M1	M2	M3	T1	T2	<A-O>	<B-O>	<M1-O>	<M2-O>	<M3-O>	<T1-O>	<T2-O>	d(OH)
[GPa]	[Å^3]	[Å^3]	[Å^3]	[Å^3]	[Å^3]	[Å^3]	[Å^3]	[Å]	[Å]	[Å]	[Å]	[Å]	[Å]	[Å]	[Å]
LDA (PAW)															
12.3	35.43	22.05	10.52	10.37	10.39	2.130	2.146	2.739	2.368	1.998	1.988	1.988	1.609	1.613	0.9746
10.6	36.43	22.34	10.62	10.48	10.48	2.137	2.155	2.759	2.379	2.005	1.995	1.995	1.610	1.615	0.9747
9.0	37.44	22.64	10.72	10.59	10.57	2.144	2.164	2.779	2.389	2.011	2.002	2.002	1.612	1.618	0.9748
7.6	38.49	22.95	10.81	10.70	10.67	2.151	2.172	2.799	2.399	2.018	2.008	2.008	1.614	1.620	0.9749
6.2	39.55	23.27	10.91	10.81	10.76	2.157	2.180	2.819	2.410	2.024	2.015	2.015	1.615	1.622	0.9751
4.9	40.65	23.59	11.01	10.92	10.85	2.164	2.188	2.838	2.421	2.030	2.022	2.021	1.617	1.624	0.9752
3.8	41.77	23.92	11.10	11.02	10.93	2.169	2.195	2.858	2.432	2.037	2.028	2.027	1.618	1.626	0.9753
2.6	42.93	24.25	11.19	11.13	11.02	2.175	2.202	2.879	2.443	2.043	2.035	2.033	1.620	1.628	0.9754
1.6	44.12	24.60	11.29	11.23	11.10	2.180	2.208	2.899	2.454	2.049	2.041	2.039	1.621	1.630	0.9755
0.6	45.36	24.96	11.38	11.34	11.18	2.185	2.214	2.920	2.466	2.055	2.048	2.045	1.622	1.632	0.9757
-0.2	46.63	25.32	11.47	11.44	11.26	2.189	2.219	2.941	2.477	2.060	2.054	2.051	1.623	1.634	0.9758
GGA (PAW)															
10.0	40.63	24.31	11.34	11.32	11.20	2.212	2.238	2.839	2.448	2.050	2.046	2.041	1.629	1.636	0.9684
8.6	41.66	24.64	11.44	11.43	11.29	2.218	2.246	2.858	2.458	2.056	2.053	2.048	1.630	1.638	0.9686
7.3	42.73	24.97	11.54	11.55	11.38	2.224	2.253	2.877	2.469	2.062	2.060	2.054	1.632	1.640	0.9688
6.1	43.81	25.30	11.64	11.66	11.47	2.230	2.261	2.895	2.480	2.069	2.067	2.060	1.633	1.642	0.9689
5.0	44.92	25.65	11.73	11.77	11.56	2.236	2.268	2.915	2.491	2.075	2.073	2.066	1.635	1.644	0.9691
4.0	46.07	26.00	11.83	11.89	11.65	2.241	2.274	2.934	2.502	2.081	2.080	2.072	1.636	1.646	0.9693
3.1	47.24	26.35	11.92	12.00	11.73	2.247	2.280	2.953	2.513	2.087	2.087	2.078	1.637	1.648	0.9694
2.2	48.45	26.72	12.02	12.11	11.81	2.251	2.286	2.973	2.525	2.093	2.093	2.084	1.638	1.650	0.9695
1.4	49.69	27.10	12.11	12.22	11.89	2.256	2.291	2.993	2.537	2.098	2.100	2.089	1.639	1.651	0.9697
0.6	50.96	27.51	12.20	12.33	11.97	2.260	2.296	3.014	2.549	2.104	2.106	2.095	1.640	1.653	0.9698
-0.1	52.27	27.93	12.29	12.44	12.05	2.264	2.301	3.035	2.562	2.110	2.113	2.101	1.641	1.654	0.9700
-0.8	53.62	28.36	12.38	12.55	12.12	2.268	2.305	3.056	2.575	2.115	2.119	2.106	1.642	1.656	0.9701

Supplementary Table 7. Polyhedral volumes (V_0) [Å^3], polyhedral bulk moduli (K_0) [GPa] and the pressure derivative of the bulk modulus (K') of tremolite at 300 K.

	T1	T2	M1	M2	M3	B	A (vacant)
LDA							
V_0	2.2	2.2	11.4	11.4	11.2	25.2	46.3
K_0	411.6	348.7	113.2	98.6	128.5	59.7	31.6
K'	7.4	4.3	6.2	5.6	5.0	6.4	3.0
GGA							
V_0	2.3	2.3	12.3	12.4	12.0	27.9	52.1
K_0	401.6	348.4	94.6	78.1	110.1	45.7	26.9
K'	5.6	2.5	7.3	6.8	6.3	7.1	3.3
Experimental results (Comodi et al., 1991)							
V_0	2.19	2.22	11.72	11.88	11.51	26.13	47.19
K_0	-	-	106.0	66.0	128.0	74.0	45.0

Supplementary Table 8. Experimentally determined elastic constants for tremolite using a reference frame where X is not parallel to the *a*-axis, but Y and Z are parallel to the *b*- and *c*-axes, respectively (Brown and Abramson, 2016). To compare this result directly with our study where X and Z are not parallel to the *a*- and *c*-axes, but Y is parallel to the *b-axis,* we have rotated the experimental elastic constants at ambient conditions.

Reference: X is not parallel to the *a*-axis, Y||*b*, and Z||*c*						
C_{ij}	1	2	3	4	5	6
1	107	47	37	0	-1	0
2	47	186	60	0	-8	0
3	37	60	232	0	-30	0
4	0	0	0	79	0	7
5	-1	-8	-30	0	48	0
6	0	0	0	7	0	50
Rotated Reference: X is not parallel to the *a*-axis, Y||*b*, and Z is not parallel to the *c*-axis						
C_{ij}	1	2	3	4	5	6
1	114	52	54	0	-14	0
2	52	186	55	0	-10	0
3	54	55	191	0	-44	0
4	0	0	0	81	0	-1
5	-14	-10	-44	0	65	0
6	0	0	0	-1	0	48

Supplementary Table 9. Pressure dependence of compressional (AV_P) and shear (AV_S) wave anisotropy of tremolite at 300 K based on LDA.

$P_{300\,K}$	[GPa]	0	1	2	3	4	5	6	7	8	9	10
AV_P	[%]	34.6	32.8	31.1	29.5	28.1	26.9	25.7	24.7	23.9	23.2	22.6
AV_S	[%]	27.5	28.6	29.7	30.8	32.0	33.1	34.2	35.4	36.5	37.6	38.8

Supplementary Table 10a. Bulk rock oxide compositions and mineral modes of the representative cratonic rock, the Kaapvaal Craton lherzolite (Griffin et al., 2009).

AV. High-T lherzolite Kaapvaal craton	
Oxides	wt%
SiO_2	44.3
TiO_2	0.17
Al_2O_3	1.74
Cr_2O_3	0.30
FeO	8.1
MnO	0.12
MgO	43.3
CaO	1.27
Na_2O	0.12
NiO	0.26
Sum	99.7
Mg#	90.5
Calculated HP database (100 km, 800 ºC)	
phase	vol%
olivine	70.6
orthopyroxene	19.8
clinopyroxene	3.5
garnet	6.1

Supplementary Table 10b. Modal proportions of mineral end members used for constructing velocity-depth profiles. We used the modal proportions for the major mineral phases reported in **Supplementary Table 10a**. Tremolite is used as a proxy for the general amphibole group.

	0% Phlogopite					
	reference	5% amph	10% amph	15% amph	20% amph	25% amph
phases	vol%	vol%	vol%	vol%	vol%	vol%
grossular	1.0	0.9	0.9	0.8	0.8	0.7
pyrope	5.1	4.9	4.6	4.4	4.1	3.8
fosterite	63.4	60.2	57.0	53.9	50.7	47.5
fayalite	7.2	6.9	6.5	6.2	5.8	5.4
enstatite	17.8	16.9	16.0	15.1	14.2	13.3
ferrosilite	2.0	1.9	1.8	1.7	1.6	1.5
diopside	3.1	3.0	2.8	2.7	2.5	2.4
hedenbergite	0.4	0.3	0.3	0.3	0.3	0.3
tremolite		5.0	10.0	15.0	20.0	25.0
phlogopite		0.0	0.0	0.0	0.0	0.0
Sum	100	100	100	100	100	100
	1% Phlogopite					
	0% amph	5% amph	10% amph	15% amph	20% amph	25% amph
phases	vol%	vol%	vol%	vol%	vol%	vol%
grossular	1.0	0.9	0.9	0.8	0.8	0.7
pyrope	5.1	4.8	4.6	4.3	4.0	3.8
fosterite	62.7	59.6	56.4	53.2	50.1	46.9
fayalite	7.2	6.8	6.4	6.1	5.7	5.4
enstatite	17.6	16.7	15.8	14.9	14.0	13.2
ferrosilite	2.0	1.9	1.8	1.7	1.6	1.5
diopside	3.1	3.0	2.8	2.6	2.5	2.3
hedenbergite	0.4	0.3	0.3	0.3	0.3	0.3
tremolite	0.0	5.0	10.0	15.0	20.0	25.0
phlogopite	1.0	1.0	1.0	1.0	1.0	1.0
Sum	100	100	100	100	100	100

Supplementary Table 11: Thermoelastic data for major mantle mineral phases.

phase	gram formula weight (g/mol)	molar volume (cm^3/ mol)	density @298K (kg/m^3)	wt% H_2O	expansivity (/K)	isothermal bulk modulus (Pa)	dK_T/dP	shear modulus (Pa)	dlnG/ dlnρ	dG/dP	first Grüneisen parameter	second Grüneisen parameter	Reference
	gfw	*V*	ρ_{298}	H_2O	a^0	K_T	K_T'	*G*	Γ	*G'*	γ_{th}	δ_T	
gr	450.40	125.40	3593	0	3.93E-05	1.64E+11	3.90	1.09E+11	5.11	1.10	1.19	4.57	*ref*[a]
py	403.09	113.20	3565	0	4.36E-05	1.67E+11	4.10	9.40E+10	4.06	1.30	1.25	5.30	*ref*[a]
fo	140.70	43.70	3222	0	6.13E-05	1.27E+11	4.20	8.16E+10	5.19	1.60	1.29	5.50	*ref*[a]
fa	203.77	46.30	4400	0	5.05E-05	1.36E+11	4.88	5.12E+10	4.69	1.71	1.21	5.40	*ref*[a]
en	200.79	62.60	3196	0	5.05E-05	1.08E+11	6.60	7.79E+10	7.55	1.90	0.95	7.55	*ref*[a]
fs	263.86	65.90	4003	0	6.32E-05	1.00E+11	6.60	5.20E+10	7.74	1.90	1.14	7.74	*ref*[a]
di	216.56	66.19	3268	0	5.70E-05	1.17E+11	4.50	7.28E+10	4.00	1.90	1.10	4.50	*ref*[a]
hed	248.09	67.95	3657	0	5.70E-05	1.21E+11	4.50	6.18E+10	6.00	1.90	1.50	6.00	*ref*[a]

ref[a]: Abers and Hacker, 2016, and the references or notes therein.

Phases: gr- grossular; py- pyrope; fo- fosterite; fa- fayalite; en- enstatite; fs- ferrosilite; di- diopside; and hed- hedenbergite.

Supplementary Figures

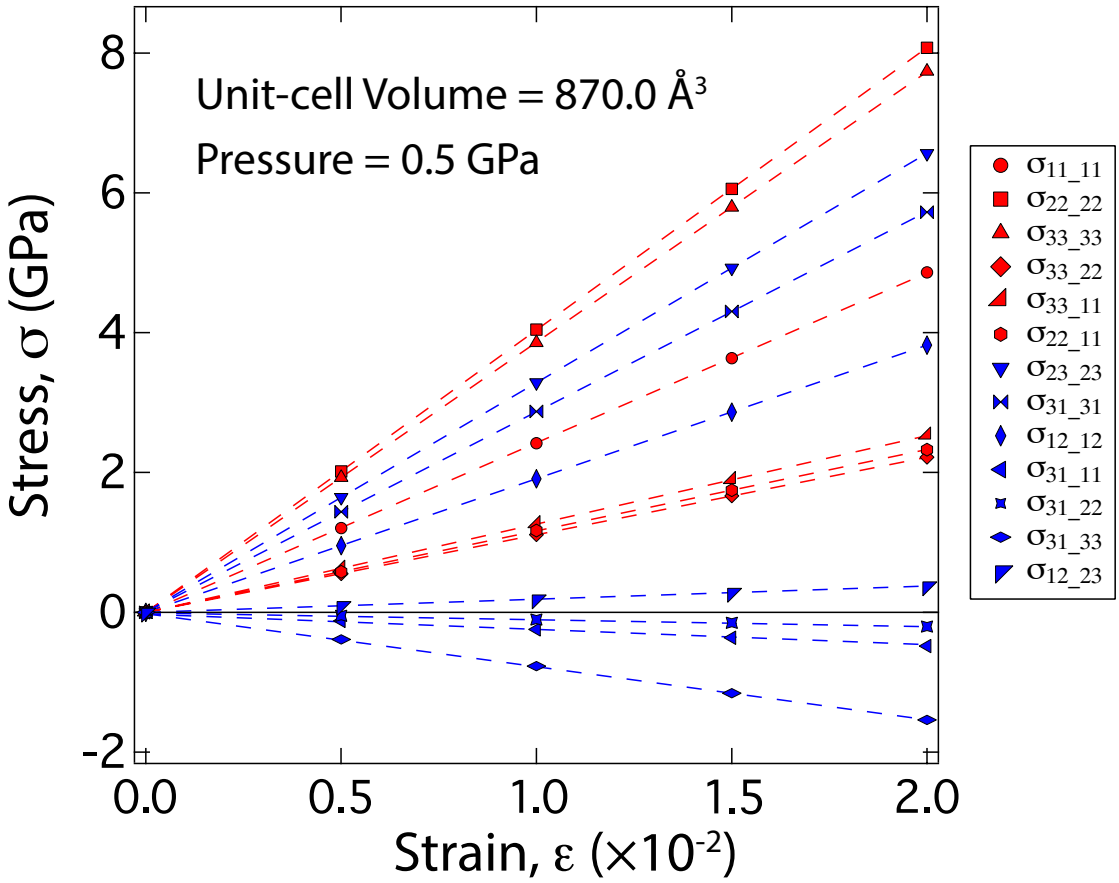

Supplementary Figure 1: Stress vs. strain relations involved in the calculation of thirteen elastic constants of tremolite. Symbols are the calculated stresses and the dashed lines represent the initial linear slopes passing through 0% and 0.5% strain, i.e., the zero strain limit. The stresses are notated with 4 indices, the first two represent the direction of stress and the last two represent the direction of applied strain. For example, σ_{ij_kl} means the difference of stresses (σ_{ij}) when we applied both positive and negative strains (ε_{kl}) by various magnitudes. The figure shows that the ±1.0% strains we applied is within the elastic limit.

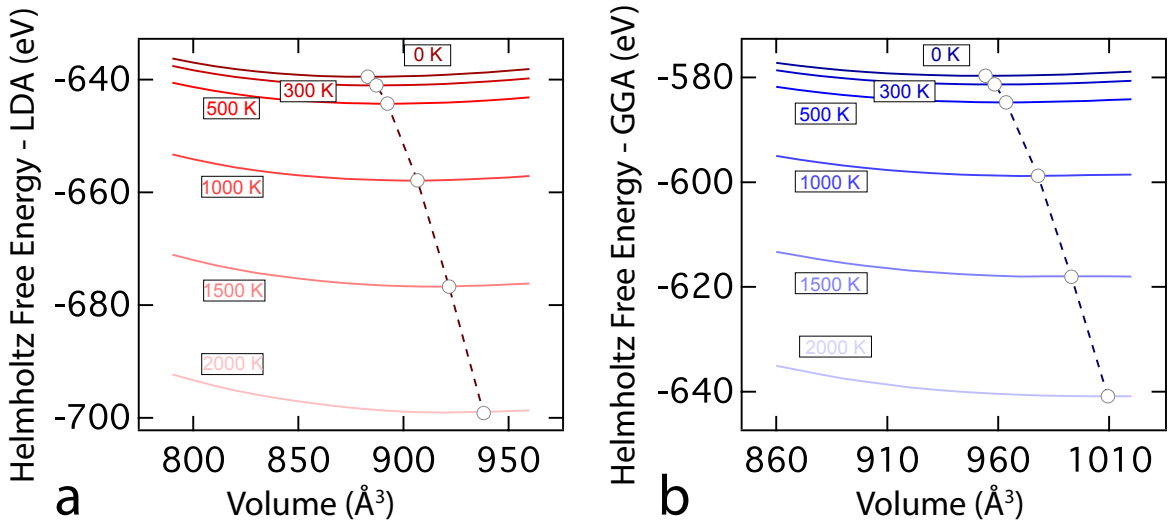

Supplementary Figure 2: Plot of Helmholtz free energy of tremolite vs. unit-cell volume for (**a**) LDA and (**b**) GGA. The temperatures are labeled. The open circles indicate the zero-pressure volume at different temperatures.

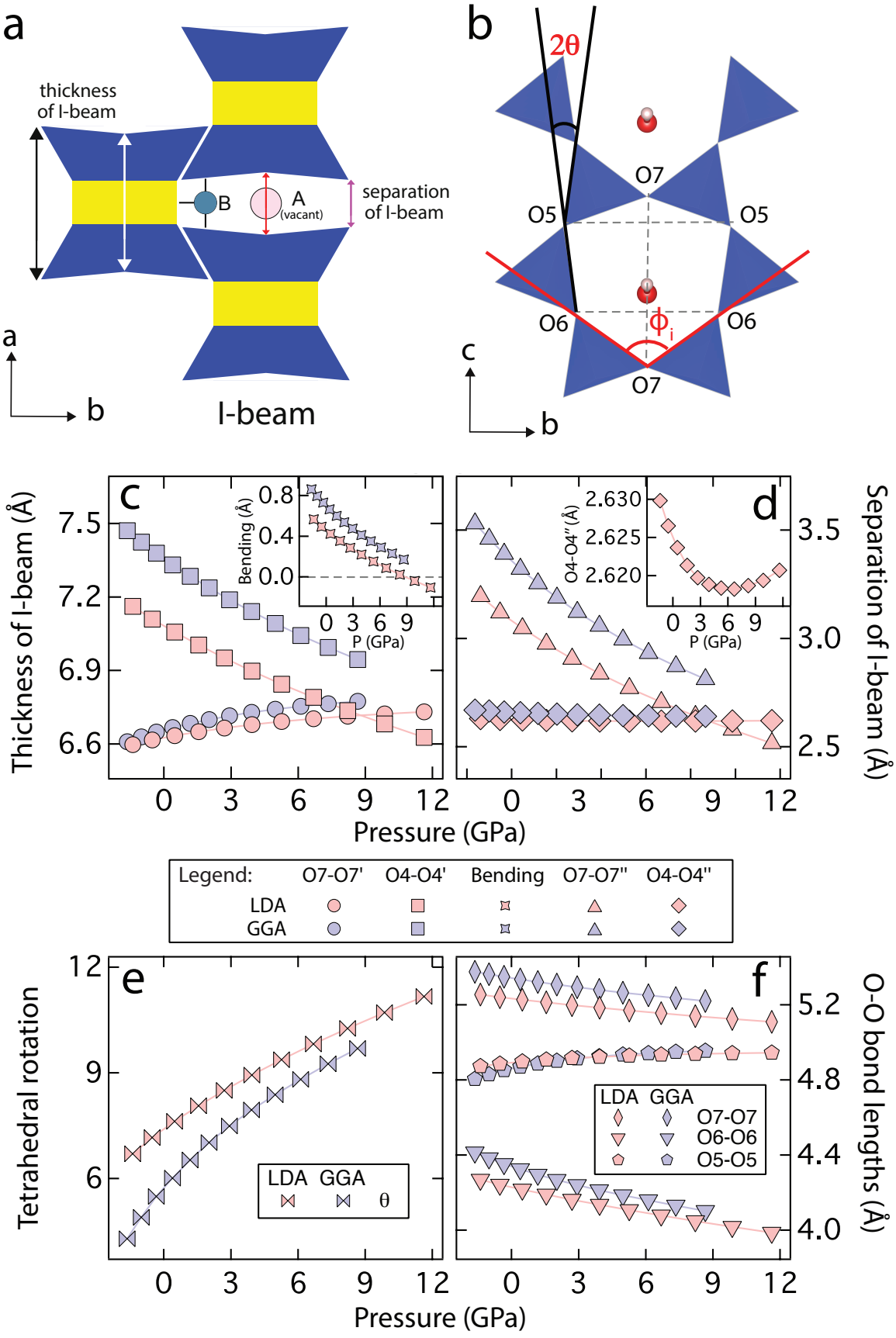

Supplementary Figure 3: (**a**) Schematic diagram of the I-beam structure in tremolite: the octahedral strip is sandwiched between two tetrahedral chains. Three I-beams are connected

together by a B site. The A site is located between the two I-beams and is vacant in tremolite. Arrows indicate the inner and outer thickness of I-beam and separation of I-beams. (**b**) Structure of the tetrahedral ring: the two tetrahedral chains parallel to the *c*-axis form ditrigonal rings. The angle θ defines the tetrahedral rotation. (**c**) Inner (O7-O7') and outer (O4-O4') thicknesses of the I-beam vs. pressure. Inset shows the pressure dependence of the bending of I-beam, i.e., the difference between the outer and inner thickness of I-beam. (**d**) Inner (O7-O7'') and outer (O4-O4'') separation of I-beam vs. pressure. Inset shows the outer separation of I-beam for LDA which shows a non-monotonic behavior. For the oxygen atom labels used in panels (**c**) and (**d**), please refer to **Figure 1** in the main draft. (**e**) Tetrahedral rotation angle vs. pressure. (**f**) Pressure dependence of the opposite basal oxygen distances of the ditrigonal ring.

References:

Abers, G.A., and Hacker, B.R. (2016) A MATLAB toolbox and Excel workbook for calculating the densities, seismic wave speeds, and major element composition of minerals and rocks at pressure and temperature. Geochemistry, Geophysics, Geosystems, 17, 616-624.

Anderson, O.L. (1984) A universal thermal equation-of-state. Journal of Geodynamics, 1, 185-214.

Anderson, O.L. (1999) The volume dependence of thermal pressure in perovskite and other minerals. Physics of the earth and planetary interiors, 112, 267-283.

Anderson, O.L., and Yamamoto, S. (1987) Interrelationship of thermodynamic properties obtained by the piston-cylinder high-pressure experiments and RPR high temperature experiments for NaCl. In Geophysical Monograph Series: High Pressure Research in Mineral Physics, edited by Manghnani, M.H., and Syono, Y., 289-298, Washington, DC.

Anderson, O.L., Isaak, D., and Oda, H. (1992) High-temperature elastic constant data on minerals relevant to geophysics. Reviews of Geophysics, 30, 57-90.

Bassett, W.A., Takahashi, T., Mao, H.K., and Weaver, J.S. (1968) Pressure-induced phase transformation in NaCl. Journal of Applied Physics, 39, 319-325.

Bina, C.R., and Helffrich, G.R. (1992) Calculation of elastic properties from thermodynamic equation of state principles. Annual Review of Earth and Planetary Sciences, 20, 527-552.

Birch, F. (1978) Finite strain isotherm and velocities for single crystal and polycrystalline NaCl at high-pressures and 300 K. Journal of Geophysical Research, 83, 1257-1268.

Brown, J.M., and Abramson, E.H. (2016) Elasticity of calcium and calcium-sodium amphiboles. Physics of the Earth and Planetary Interior, 261, 161-171.

Duffy, T.S., and Anderson, D.L. (1989) Seismic velocities in mantle minerals and the mineralogy of the upper mantle. Journal of Geophysical Research: Solid Earth, 94, 1895-1912.

Fei, Y., Mao, H.K., Shu, J., and Hu, J. (1992) P-V-T equation of state of magnesiowüstite $(Mg_{0.6}Fe_{0.4})O$. Physics and Chemistry of Minerals, 18, 416-422.

Griffin, W.L., O'reilly, S.Y., Afonso, J.C., and Begg, G.C. (2008) The composition and evolution of lithospheric mantle: a re-evaluation and its tectonic implications. Journal of Petrology, 50, 1185-1204.

Hacker, B.R., and Abers, G.A. (2004) Subduction Factory 3: An Excel worksheet and macro for calculating the densities, seismic wave speeds, and H_2O contents of minerals and rocks at pressure and temperature. Geochemistry, Geophysics, Geosystems, 5, Q01005.

Hashin, Z., and Shtrikman, S. (1962) On some variational principles in anisotropic and nonhomogeneous elasticity. Journal of the Mechanics and Physics of Solids, 10, 335-342.

Holland, T.J.B., and Powell, R. (1998) An internally consistent thermodynamic data set for phases of petrological interest. Journal of metamorphic Geology, 16, 309-343.

Litasov, K.D., Fei, Y., Ohtani, E., Kuribayashi, T., and Funakoshi, K. (2008) Thermal equation of state of magnesite to 32 GPa and 2073 K. Physics of the Earth and Planetary Interiors, 168, 191-203.

Litasov, K.D., Ohtani, E., Ghosh, S., Nishihara, Y., Suzuki, A., and Funakoshi, K. (2007) Thermal equation of state of superhydrous phase B to 27 GPa and 1373 K. Physics of the Earth and Planetary Interiors, 164, 142-160.

Nishihara, Y., Nakayama, K., Takahashi, E., Iguchi, T., and Funakoshi, K.Ì. (2005) P-V-T equation of state of stishovite to the mantle transition zone conditions. Physics and Chemistry of Minerals, 31, 660-670.